RSC Advances

PAPER

View Article Online
View Journal | View Issue

Cite this: *RSC Adv.*, 2016, **6**, 19288

Strategy to improve phase compatibility between proton conductive $BaZr_{0.8}Y_{0.2}O_{3-\delta}$ and nickel oxide†

Donglin Han,*[a] Yuki Otani,[a] Yohei Noda,[ab] Takayuki Onishi,[a] Masatoshi Majima[b] and Tetsuya Uda*[a]

Received 16th December 2015
Accepted 10th February 2016

DOI: 10.1039/c5ra26947d

www.rsc.org/advances

$BaZr_{0.8}Y_{0.2}O_{3-\delta}$ (BZY20) is a promising candidate as an electrolyte in protonic ceramic fuel cells (PCFCs), and nickel (Ni) is known to show good electrode properties for the anode reaction. However, their compatibility seems to be questionable, since during the co-sintering process for cell fabrication, a second phase of BaY_2NiO_5 formed due to a reaction between BZY20 and NiO. The results in this work revealed that BaY_2NiO_5 was unstable against high temperature (1500 and 1600 °C), and could also be reduced in a hydrogen atmosphere at 600 °C. The products of these reactions may affect fuel cell performance. A systematic work was then performed to provide fundamental insight into the reactivity between BZY20 and NiO, which was found to be impacted significantly by the compositional homogeneity of the BZY20 powder used for cell fabrication, and also the BaO activity during the co-sintering process. It is concluded that improving the compositional homogeneity of BZY20, by elevating the final heating temperature for BZY20 from 1300 to 1600 °C in this work, and choosing a proper sintering strategy may improve effectively the phase purity of the cell.

1. Introduction

Y-Doped $BaZrO_3$ (BZY) is an attractive material due to its high protonic conductivity in a humid atmosphere.[1–3] Incorporation of BZY into fuel cells as an electrolyte therefore seems to be quite promising, since the operation temperature can thereby be decreased to an intermediate temperature range (450–700 °C), lower than that of conventional solid oxide fuel cells (SOFCs) using oxide ion conductive electrolytes (around 750–1000 °C).[4,5] Great efforts have been devoted to the development of BZY electrolyte-based fuel cells.[6–13] However, a lot of challenges still remain. Referring to the anode, it is regarded to be a good choice to use a composite one (generally, a mixture of nickel oxide (NiO) and the corresponding electrolyte material) which has already been widely applied in the SOFC community.[5] The same strategy has also been introduced into the BZY electrolyte-based fuel cells with prospective applicability.[8–14]

However, during the co-sintering process for fuel cell fabrication, a second phase of BaY_2NiO_5 formed due to the reaction between BZY and NiO.[14–16] Although a positive role of BaY_2NiO_5 in improving sinterability of BZY was suggested by Tong *et al.*,[17] a recent work by Fang *et al.* reported that such second phase decomposed in reducing or humid environment at 900 °C.[15] Since H_2 will be fed to the anode, existence of BaY_2NiO_5 is rather unfavorable, whose decomposition introduces electrochemical insulator phase (Y_2O_3), and also potentially results in cracks or delamination in the anode.[15] However, although BaY_2NiO_5 formed after heating BZY–NiO mixture at 1400 °C, its existence was not confirmed by elevating the temperature to 1600 °C.[18] Such information suggests the possibility to suppress the formation of BaY_2NiO_5. But first of all, it is necessary to perform a detailed investigation on the behavior of BaY_2NiO_5 at high temperature, and also the reaction between BZY and NiO. We therefore conducted this work.

2. Experimental

2.1 Material preparation

Samples of $BaZr_{0.8}Y_{0.2}O_{3-\delta}$ (BZY20) and BaY_2NiO_5 were prepared by a conventional solid state reaction method. Starting materials ($BaCO_3$, ZrO_2 and Y_2O_3 for $BaZr_{0.8}Y_{0.2}O_{3-\delta}$, and $BaCO_3$, Y_2O_3 and NiO for BaY_2NiO_5) were mixed at the desired ratios, and ball-milled for 24 h. Mixtures were then pressed into pellets under 9.8 MPa and heat-treated at 1000 °C in ambient atmosphere for 10 h. After ball-milling for 10 h, the samples were pressed into pellets under 9.8 MPa again, and kept at 1300 °C in ambient atmosphere for 10 h for synthesizing. The as-synthesized samples were ball-milled for 100 h and 24 h for BZY20 and BaY_2NiO_5,

[a]*Department of Materials Science and Engineering, Kyoto University, Yoshida Honmachi, Sakyo-ku, Kyoto 606-8501, Japan. E-mail: han.donglin.8n@kyoto-u.ac.jp; uda_lab@aqua.mtl.kyoto-u.ac.jp; Fax: +81-75-753-5284; Tel: +81-75-753-5445*

[b]*Sumitomo Electric Industries, Ltd., 1-1-1, Koyakita, Itami-shi, Hyogo 664-0016, Japan*

† Electronic supplementary information (ESI) available. See DOI: 10.1039/c5ra26947d

respectively. The BaY_2NiO_5 powder was pressed at 392 MPa to prepare pellet-like samples. For all the heat-treatments in this work, the heating rates from room temperature to 1000 °C, and 1000 °C to higher temperature (1300, 1400, 1500 and 1600 °C) were 4.17 and 3.33 °C min^{-1}, respectively.

The as-synthesized BZY20 powder was pressed into pellets at 392 MPa. After being embedded in sacrificial powder with the composition of the as-synthesized BZY20, these BZY20 pellets were heated at 1600 °C for 24 h in oxygen atmosphere for sintering. The as-sintered BZY20 was pulverized by ball-milling for 50 h. For the sake of clarity, BZY20 with the final heating temperature of 1300 and 1600 °C are named as BZY20 (1300 °C) and BZY20 (1600 °C), respectively, in this work. Then, both BZY20 (1300 °C) and BZY20 (1600 °C) were mixed with 70 wt% NiO, and ball-milled for 10 h for mixing. The mixture was then pressed at 392 MPa to form pellet-like samples.

2.2 Sintering strategy

With the purpose to create environment containing different BaO activity during the sintering process, as shown in Fig. 1, different strategies were attempted for sample setting. To evaluate the stability of BaY_2NiO_5 at 1500 and 1600 °C, a method as shown in Fig. 1(a) with the name of open-sintering was used. Magnesia (MgO) containers were inserted between the BaY_2NiO_5 pellet-like samples and alumina (Al_2O_3) plate-like crucibles to prevent their direct touch and unfavorable reaction. In addition to the open-sintering, two other methods named as cover-sintering (Fig. 1(b)) and embed-sintering (Fig. 1(c)) were also applied to evaluate the reactivity between BZY20 and NiO by heat-treating the BZY20–70 wt% NiO pellet-like samples. In the cover-sintering method, the BZY20–70 wt% NiO pellet-like samples were covered with Al_2O_3 caps. Sacrificial powder (BZY20 (1300 °C)–10 wt% $BaCO_3$) was added to prevent a direct touch of the samples from the Al_2O_3 plate-like crucibles, and also seal the space between the Al_2O_3 caps and the plate-like crucibles in certain degree. In the embed-sintering method, the samples were embedded in sacrificial powder (only BZY20) in the MgO containers. After heat-treatment, the BaY_2NiO_5 and BZY20–70 wt% NiO pellet-like samples were all quenched in the ambient atmosphere.

2.3 Characterization

X-ray diffraction (XRD) measurements were performed using Cu Kα radiation with X'Pert-ProMPD (PANalytical, Almelo, Netherland). Rietveld refinement was carried out utilizing a commercial software X'Pert HighScore Plus to simulate the XRD patterns. Microstructures were observed by scanning electron microscopy (SEM) with VE-7800 (Keyence Co., Osaka, Japan) and scanning transmission electron microscopy (STEM) with JEM-2100F (JEOL, Tokyo, Japan). Energy dispersion X-ray spectroscopy with Genesis-XM2 (SEM-EDS, EDAX, Mahwah, NJ) and also JED-2300 (STEM-EDS, JEOL, Tokyo, Japan) were used for composition measurement.

3. Results

3.1 Stability of BaY_2NiO_5 in H_2 and O_2 atmospheres

As shown in Fig. 2(a), the as-synthesized BaY_2NiO_5 sample was a single phase after the heat-treatment at 1300 °C. The single

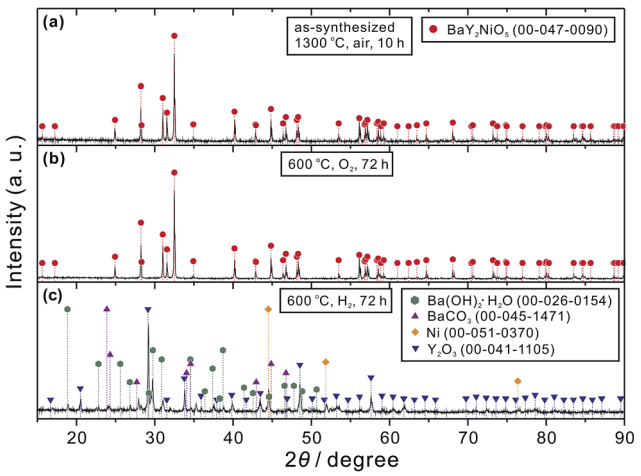

Fig. 2 Powder XRD patterns of (a) as-synthesized BaY_2NiO_5 after heat-treatment at 1300 °C in air for 10 h, then heat-treated at 600 °C in (b) dry O_2, or (c) dry H_2 atmosphere for 10 h. BaY_2NiO_5 powder was used in the heat-treatment at 600 °C in dry O_2 and H_2. XRD patterns were collected in ambient atmosphere after each heat-treatment. The reported reference patterns of BaY_2NiO_5 (JCPDS no. 00-047-0090), $Ba(OH)_2 \cdot H_2O$ (JCPDS no. 00-026-0154), $BaCO_3$ (JCPDS no. 00-045-1471), Ni (JCDPS no. 00-051-0370), and Y_2O_3 (JCPDS no. 00-041-1105) are also plotted.

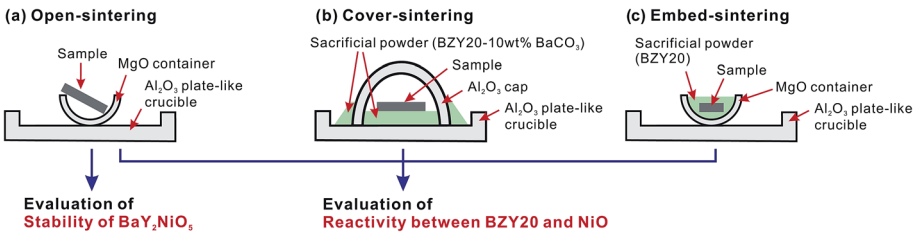

Fig. 1 Schematics of methods for sample setting in this work. For evaluating the stability of BaY_2NiO_5 and reactivity between BZY20 and NiO, three different methods, namely (a) open-sintering, (b) cover-sintering and (c) embed-sintering, were adopted. In order to prevent the reaction between Al_2O_3 and BaY_2NiO_5, MgO containers were used in the open-sintering and embed sintering methods to avoid direct touch between the samples and the Al_2O_3 plate-like crucible.

phase was also confirmed after keeping the sample powder at 600 °C in dry O_2 atmosphere for 72 h (Fig. 2(b)). However, when the atmosphere was changed to dry H_2, as shown in Fig. 2(c), BaY_2NiO_5 decomposed completely (eqn (1)). Since the sample was lately exposed to the ambient atmosphere containing H_2O and CO_2 for the XRD measurements, $Ba(OH)_2 \cdot H_2O$, $BaCO_3$ were identified. Such result agrees with that reported by Fang *et al.* by heating BaY_2NiO_5 at 900 °C in dry H_2.[15]

$$BaY_2NiO_5 + H_2(g) \xrightarrow{600\ ^\circ C} Ba(OH)_2 + Y_2O_3 + Ni \quad (1)$$

3.2 Stability of BaY_2NiO_5 at 1500 and 1600 °C

In order to evaluate the behaviour at 1500 and 1600 °C, BaY_2NiO_5 pellet-like samples were heat-treated at these temperatures in ambient atmosphere for desired time, and finally quenched. It is worth noting here that at first, we placed the samples directly on Al_2O_3 plate-like crucibles, but found that BaY_2NiO_5 reacted with Al_2O_3 to form $BaAl_2O_4$ and $Ba_3Y_2AlO_{7.5}$ at 1500 and 1600 °C (detailed information is given in Fig. S1 to S3†). In order to prevent such reaction, we then used MgO containers to accommodate the BaY_2NiO_5 samples (a schematic as shown in Fig. 1(a)). As shown in Fig. 3, when heating at 1500 °C, the samples kept the round pellet-shape, and no obvious change in their appearance was confirmed. However, when heating at 1600 °C, although the shape of the pellets can still be identified, it is obvious that black liquid-like product formed, which further spread over the entire surface of the MgO containers with the heating time increased to 2 h. After the sample was heated for 24 h, such black liquid-like product disappeared, and the MgO crucibles showed green appearance possibly due to the diffusion of Ni inward.

These residues of BaY_2NiO_5 pellet-like samples were pulverized and analysed by powder XRD. As shown in Fig. 4, when heating at 1500 °C for 0 h (quenched immediately after heating up to 1500 °C) and 1 h, only the diffraction peaks belonging to the BaY_2NiO_5 single phase were observed. When the sample was kept at 1500 °C for 2 h, diffraction peaks of Y_2O_3 appeared. And the intensity of Y_2O_3 peaks further increased with the heating time extended to 5 and 24 h. These results suggest that at 1500 °C, BaY_2NiO_5 is still a solid phase. However, theoretical calculation based on reported thermodynamic data[19–21] reflects the fact that Ba and Ni oxides and hydroxides have relatively high partial pressure at high temperature, as shown in Fig. 5. For example, the partial pressure of $Ba(OH)_2$ was calculated to be as high as 7.32×10^{-5} atm at 1500 °C, if the reaction among BaO(s), H_2O(g) (partial pressure assumed as 0.01 atm), and $Ba(OH)_2$(g) reached equilibrium. Such volatile property of Ba and Ni oxides and hydroxides results in a gradual decomposition of BaY_2NiO_5, with Y_2O_3 remained (eqn (2)).

$$BaY_2NiO_5(s) \xrightarrow{1500\ ^\circ C} Y_2O_3(s) + BaO(g) + NiO(g) \quad (2)$$

The case for heating at 1600 °C is different. As shown in Fig. 6(a), even the sample was just heated up to 1600 °C, in addition to BaY_2NiO_5, diffraction peaks belonging to Y_2O_3 and

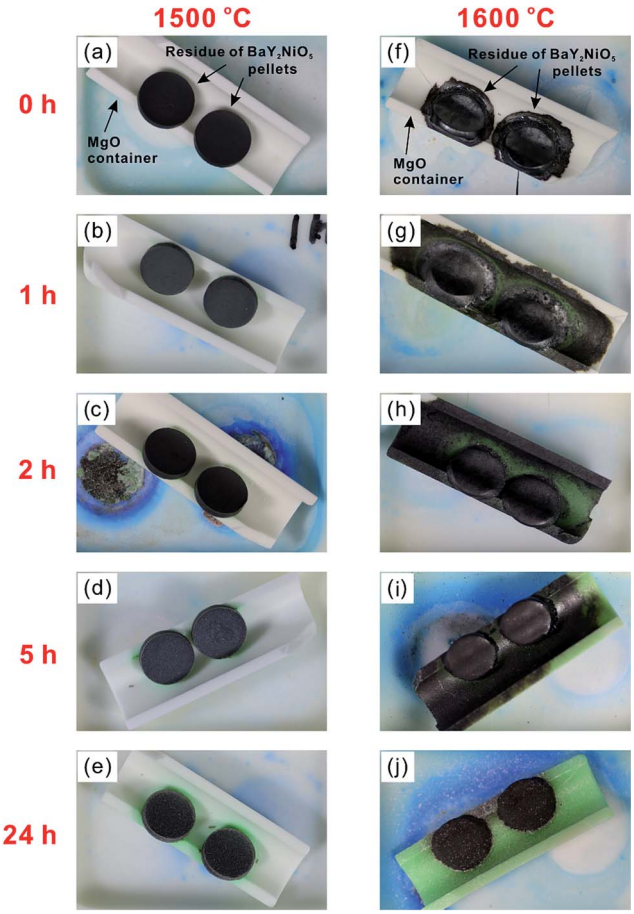

Fig. 3 Optical images of BaY_2NiO_5 pellets heat-treated at 1500 and 1600 °C in ambient atmosphere for various time. The BaY_2NiO_5 pellets were placed on MgO containers, which were placed on Al_2O_3 plate-like crucibles, the same as shown in Fig. 1(a). Blue residue on the Al_2O_3 plate-like crucibles was due to past experiments. The heating rates from room temperature to 1000 °C, and 1000 °C to 1500 or 1600 °C were 4.17 and 3.33 °C min^{-1}, respectively. All the pellets were finally quenched in ambient atmosphere.

$BaNiO_2$ appeared. When the sample was heated for 24 h, the $BaNiO_2$ peaks disappeared. Such results suggest a totally different phase relationship at 1600 °C, compared with the case at 1500 °C. SEM-EDS analysis was then performed on the sample heated at 1600 °C for 0 h (quenched immediately after heating up to 1600 °C). As shown in Fig. 7(a), the area marked with number 1 and 2 has the composition close to BaY_2NiO_5 (detailed SEM-EDS point analysis results are given in Table S1†), whereas some adjacent areas (point 6) is compositionally Y-rich, indicating possible existence of Y_2O_3. The areas with the composition close to $BaNiO_2$ (points 4 and 5) showed a clear liquid-like appearance with some small precipitates embedded (a SEM image with large magnification is given in Fig. 7(b)). However, we did not succeed in determining the composition of these precipitates by SEM-EDS, because they are too small. Since the shape of the round pellets can still be identified even after heating for 24 h (Fig. 3(f)–(j)), it is reasonable to believe that at 1600 °C, BaY_2NiO_5 do not melt, but peritectically decomposed to Y_2O_3 and a liquid phase, as given in eqn (3). But during

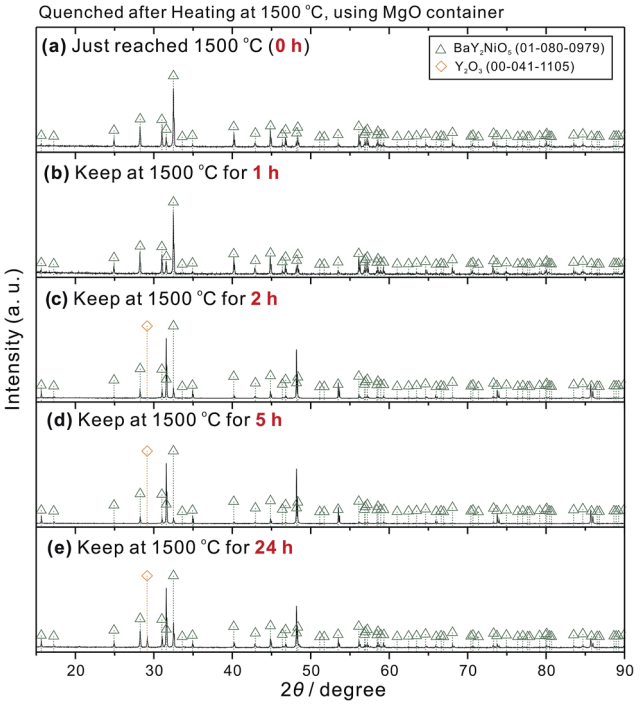

Fig. 4 Powder XRD patterns of the residues of BaY_2NiO_5 pellet-like samples heat-treated at 1500 °C for various time. The pellets were placed on MgO containers, which were placed on Al_2O_3 plate-like crucibles (Fig. 1(a)). The heating rates from room temperature to 1000 °C, and 1000 °C to 1500 °C were 4.17 and 3.33 °C min^{-1}, respectively. All the pellets were finally quenched in ambient atmosphere.

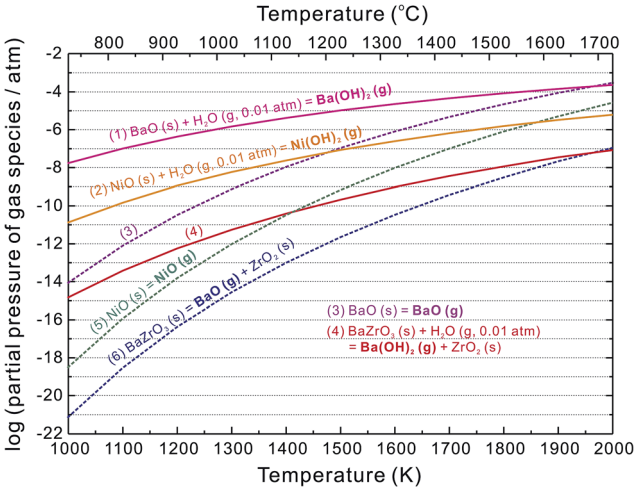

Fig. 5 Theoretical calculation of partial pressure of BaO, NiO, $Ba(OH)_2$, $Ni(OH)_2$ against temperature based on the reported thermodynamic data.[19–21] The partial pressure of water vapor was assumed to be 0.01 atm.

the quenching from 1600 °C, the liquid phase decomposed to $BaNiO_2$ and the small precipitates (eqn (4)). Based on previous reports on relevant systems,[22–25] we here propose a schematic pseudoternary phase diagram of BaO–$YO_{1.5}$–NiO at 1600 °C (Fig. 8), in which a qualitative indication of the phase

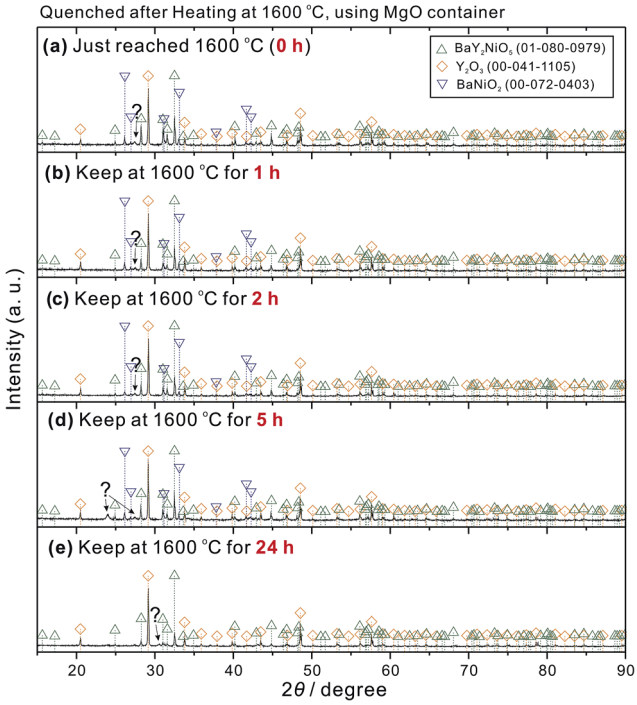

Fig. 6 Powder XRD patterns of the residues of BaY_2NiO_5 pellet-like samples heat-treated in ambient atmosphere at 1600 °C for various time. The pellets were placed on MgO containers, which were placed on Al_2O_3 plate-like crucibles (Fig. 1(a)). The heating rates from room temperature to 1000 °C, and 1000 °C to 1600 °C were 4.17 and 3.33 °C min^{-1}, respectively. All the pellets were finally quenched in ambient atmosphere. Some small peaks unable to be identified are marked with question marks.

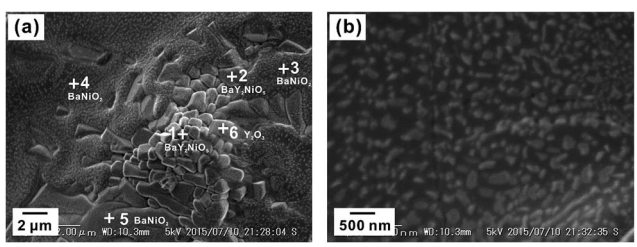

Fig. 7 (a) A SEM image of the surface of the BaY_2NiO_5 pellet heat-treated in ambient atmosphere at 1600 °C for 0 h (the sample was quenched in ambient atmosphere just after heating up to 1600 °C). Remaining of BaY_2NiO_5 (points 1 and 2), and existence of $BaNiO_2$ (points 3, 4 and 5), and Y_2O_3 (point 6) were confirmed by SEM-EDS point analysis. The detailed composition of each point was listed in Table S1.† The morphology of the areas with the composition close to $BaNiO_2$ (points 4 and 5) was shown in (b) with large magnification.

relationship was given. Anyhow, quantitative determination of the phase boundary might be an interesting topic in the future.

$$BaY_2NiO_5 \xrightarrow{1600\ ^\circ C} Y_2O_3(s) + \text{liquid phase} \quad (3)$$

$$\text{liquid phase} \xrightarrow{\text{cooling from } 1600\ ^\circ C} BaNiO_2(s) + \text{small precipitates}(s) \quad (4)$$

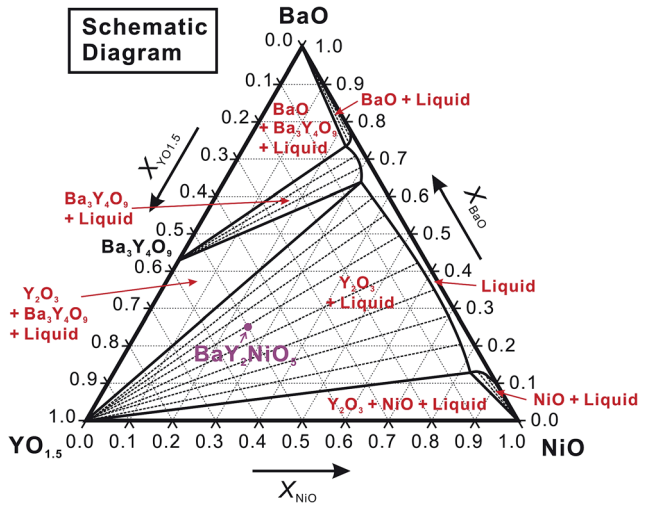

Fig. 8 A schematic pseudoternary phase diagram of $BaO–YO_{1.5}–NiO$ system at 1600 °C based on previous reports on the relevant systems.[22–25] The phase relationship is established based on the experimental results of the present work, but a more detailed investigation is expected in future to determine the precise phase boundary.

3.3 Dependence of BZY20–NiO reactivity on final heating temperature of BZY20

It is thereby an interesting and also important topic that under what kind of conditions would BaY_2NiO_5 form in the anode. Pellet-like samples with the composition of BZY20 : NiO = 30 : 70 wt% were heated in ambient atmosphere at the temperature range of 800 to 1600 °C for 10 h with the open-sintering method (Fig. 1(a)). Both the BZY20 powders finally heat-treated at 1300 and 1600 °C were used. As shown in Fig. 9(a), for the BZY20 (1300 °C)–70 wt% NiO mixture, peaks belonging to Y_2O_3 appeared even after heating at 800 and 900 °C, possibly due to the improvement of crystallinity of the Y_2O_3 residue. When the temperature was elevated to 1000 °C, the Y_2O_3 peaks disappeared, whereas those of BaY_2NiO_5 appeared. The existence of BaY_2NiO_5 was confirmed from 1000 to 1400 °C. In addition, at 1400 °C, the peaks of Y_2O_3 rose again to co-exist with those of BaY_2NiO_5. When the temperature was further increased to 1500 and 1600 °C, BaY_2NiO_5 disappeared. Only the Y_2O_3 peaks were observed.

However, the mixture added with the BZY20 powder finally heated at 1600 °C behaved in a different way. As shown in Fig. 9(b), no second phase was confirmed when the sample was heat-treated from 800 to 1100 °C. The peaks belonging to BaY_2NiO_5 appeared only with the temperature elevated to 1200 and 1300 °C. Further heating at 1400–1600 °C results in the formation of Y_2O_3, but BaY_2NiO_5 disappeared.

The XRD patterns were simulated by Rietveld refinement to estimate weight amounts of the second phases. As shown in Fig. 10, when BZY20 (1300 °C) was added, the weight amount of BaY_2NiO_5 was larger than 3 wt% after heating at 1000–1200 °C, and decreased with the increasing temperature higher than 1200 °C. However, using BZY20 (1600 °C) powder did not only lead to a relatively narrow temperature range for BaY_2NiO_5 confirmation (1200–1300 °C), and also reduced the BaY_2NiO_5 amount (1.1 and 1.7 wt% at 1200 and 1300 °C, respectively). In addition, in both the two cases, Y_2O_3 appeared at 1400 °C, with its amount increased with the elevating temperature.

Variation of lattice constants of the perovskite phase (BZY20) in the BZY20–70 wt% NiO mixture is shown in Fig. 11. It is clear that without adding NiO, the lattice constant of BZY20 finally heat-treated at 1300 °C is smaller than that heat-treated at 1600 °C. The lattice constant of the perovskite phase in BZY20 (1600 °C)–70 wt% NiO decreased with the increasing heating temperature, due to diffusion of Ni cations into the BZY20 lattice, accompanied by an intra-grain Ba-loss.[3] But the lattice constant of the perovskite phase in BZY20 (1300 °C)–70 wt% NiO increased slightly with the increasing temperature, which is regarded to be a combined effect from the Ni diffusion (shrinking the lattice) and improvement in compositional homogeneity (expanding the lattice). The status of the perovskite phase in these two samples seems to get approached after heating at 1500 °C for 10 h, since the lattice constants was very close. However, after heating at 1600 °C, the lattice constant of the perovskite phase in BZY20 (1600 °C)–70 wt% NiO is relatively small, compared with that that in BZY20 (1300 °C)–70 wt% NiO. It is attributed to a more severe Ba-loss in the open-sintering mode at such high temperature (1600 °C), and also a more significant segregation of Y_2O_3 (as shown in Fig. 10).

3.4 STEM-EDS analysis on BZY20 finally heat-treated at 1300 and 1600 °C

In our previous works, we supposed that the status of BZY20 is different after finally heating at 1300 and 1600 °C due to an obvious difference in lattice constant.[18,26] Moreover, it is a very common method to fabricate the anode by mixing NiO with as-synthesized BZY20.[8–14] And 1300 °C is a typical synthesizing temperature for using solid state reaction method to synthesize BZY20.[26–32] So, a detailed analysis of the as-synthesized BZY20 after heating at 1300 °C is highly necessary.

Fang *et al.*[33] suggested that by mechanical mixing (such as ball-mill in this work), it was difficult to achieve a homogeneous mixing of the raw materials of $BaCO_3$, ZrO_2 and Y_2O_3. It seems to be true, since we confirmed the residue of these raw materials in BZY20 heat-treated at 1300 °C by STEM observation, as shown in Fig. 12 (although these residues were not observed from XRD patterns (Fig. S4†)). However, such raw material residue was not observed in the sample heat-treated at 1600 °C. Elevating the final heating temperature from 1300 to 1600 °C decreased effectively the residue of raw materials, raising a great difference between BZY20 (1300 °C) and BZY20 (1600 °C).

Fig. 13(a) shows a bright field STEM (BF-STEM) image of the perovskite phase area in BZY20 (1300 °C), which exhibits a different morphology from that containing residue of raw materials (Fig. 12). Then, STEM-EDS point analysis of several different areas was performed to determine the local composition of such perovskite phase (examples for the STEM-EDS analysis are given in the ESI†). As shown in Fig. 13(c) ($BaCO_3$,

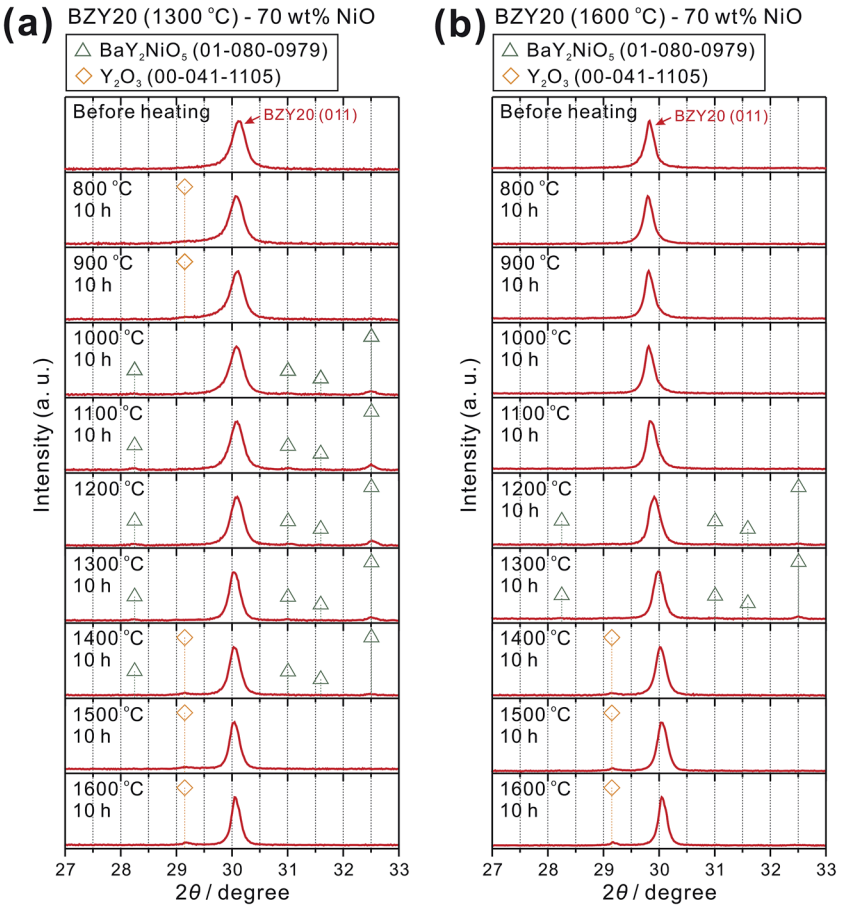

Fig. 9 Powder XRD patterns between 27 and 33 degree of the BZY20–70 wt% NiO mixtures. The BZY20 powder added was finally heat-treated at (a) 1300 °C in ambient atmosphere for 10 h, and (b) 1600 °C in O_2 for 24 h, respectively. These samples were kept in ambient atmosphere at the desired temperature between 800 and 1600 °C for 10 h using the open-sintering method (Fig. 1(a)). The heating rates in the temperature ranges of room temperature to 1000 °C, and 1000 °C to 1600 °C were 4.17 and 3.33 °C min^{-1}, respectively. All the samples were finally quenched in ambient atmosphere.

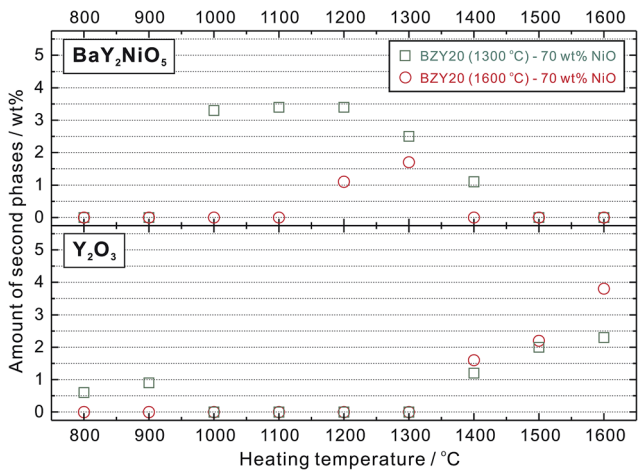

Fig. 10 Weight amount (wt%) of the second phases (BaY_2NiO_5 and Y_2O_3) generated after heat-treatment at various temperature. The weight amount was estimated by Rietveld refinement to simulate the powder XRD patterns shown in Fig. 9.

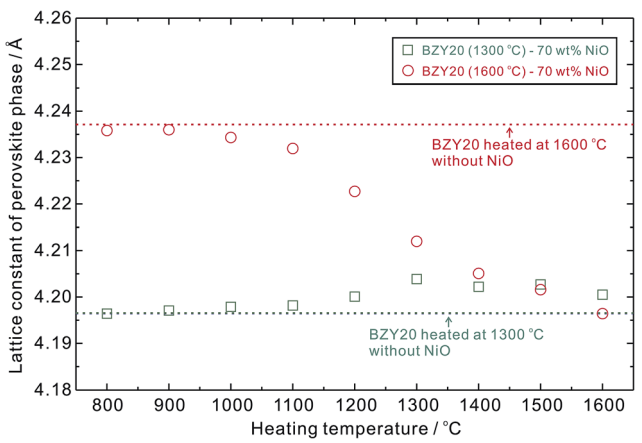

Fig. 11 Lattice constants of the perovskite phase in the mixture of BZY20 and NiO after heat-treated at the desired temperature between 800 and 1600 °C in ambient atmosphere for 10 h, using the open-sintering method (Fig. 1(a)). All the samples were finally quenched in the ambient atmosphere after the heat-treatment.

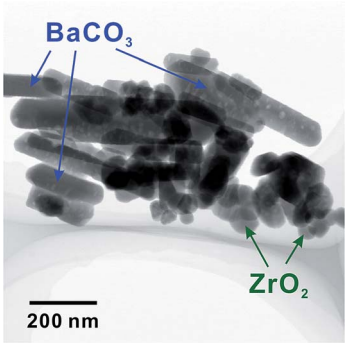

Fig. 12 A bright field STEM (BF-STEM) image of BZY20 powder heat-treated at 1300 °C for 10 h with a subsequent ball-milling for 100 h to pulverize. The large long grains and small round grains were determined to be $BaCO_3$ and ZrO_2, respectively, by STEM-EDS point analysis.

Y_2O_3 and ZrO_2 residues were excluded), a very obvious compositional scattering, especially in the Y content, can be seen. A quite significant amount of the analyzing points locate in the area where the Y content is lower than the nominal value, and existence of highly Y-rich grains was also detected. Such result clearly indicates that the cation distribution in the as-synthesized BZY20 is not so homogeneous, possibly due to the insufficient diffusion of cations to achieve a uniform distribution under the current synthesizing condition (1300 °C for 10 h) or different phase relationship at 1300 °C. And we consider that such compositional imhomogeneity should be the reason why the peak shape of BZY20 (1300 °C) is broad and asymmetric, and its lattice constant is smaller than that of BZY20 (1600 °C).[18,23] In contrary, for BZY20 finally heat-treated at 1600 °C (a BF-STEM image is shown in Fig. 13(b) for the powder sample after ball-milling), significantly improved homogeneity in composition was confirmed by STEM-EDS. As shown in Fig. 13(d), most of the grains analyzed were

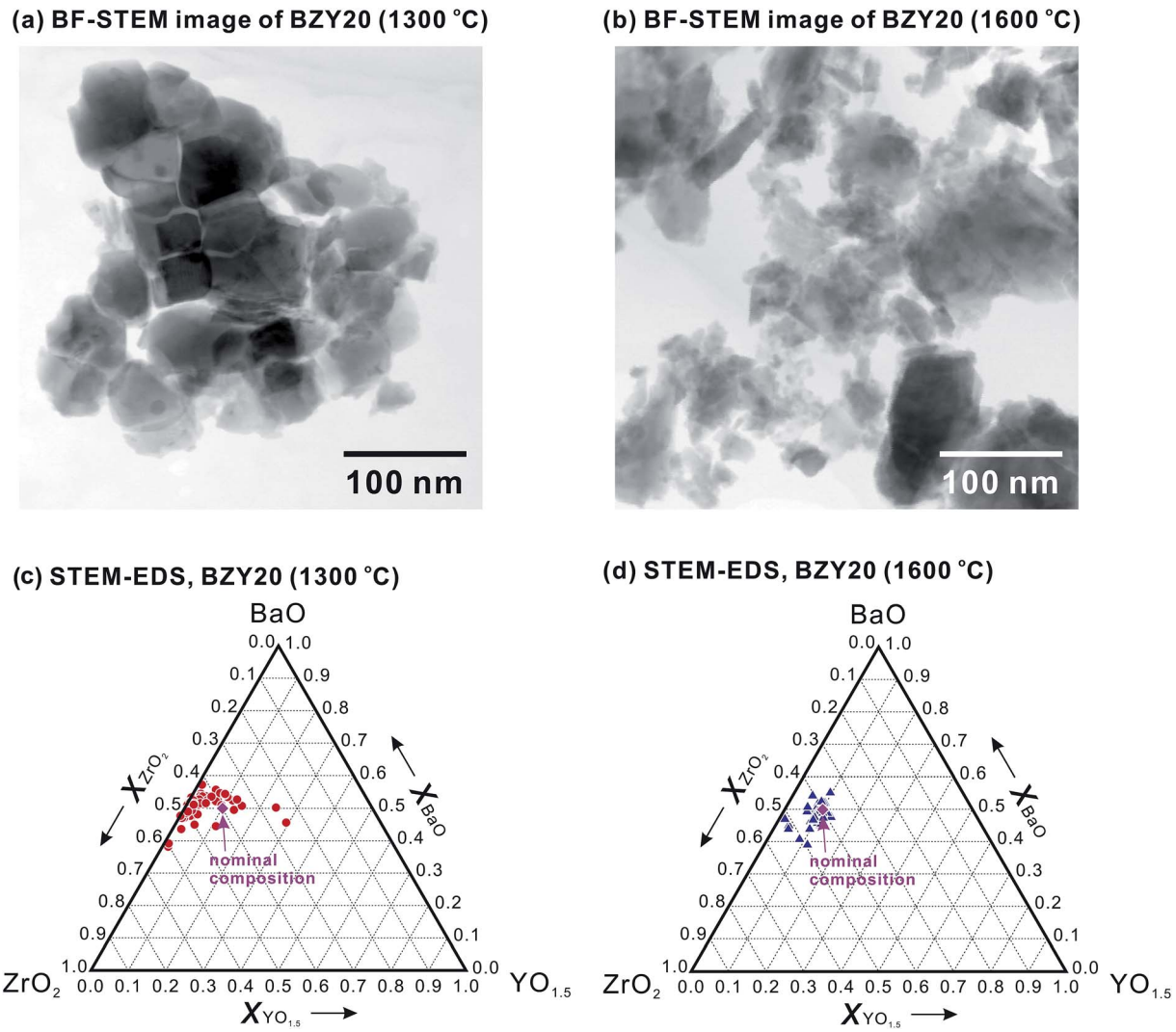

Fig. 13 BF-STEM images of grains belonging to perovskite phases in BZY20 finally heat-treated at (a) 1300 °C for 10 h in ambient atmosphere, and (b) 1600 °C for 24 h in O_2. STEM-EDS point analysis was applied to determine local compositions of these powder samples with the final heating temperature of (c) 1300 °C (d) 1600 °C. The position for nominal composition is indicated by a purple diamond symbol.

determined to have the composition close to the nominal one. Although some grains are detected to be compositionally deviated from the nominal value, but the amount is very small. Such improvement in compositional homogeneity agrees well with our previous work.[27] The difference in compositional homogeneity is a quite interesting and important factor.

It is thereby definite that the final heating temperature of BZY20 (1300 or 1600 °C), which greatly influence the status of BZY20 (compositional homogeneity, residue of the starting materials, *etc.*), makes BZY20 to show different reactivity with NiO.

3.5 Dependence of BZY20–NiO reactivity on BaO activity

With the aim to control the BaO activity during sintering, different sintering strategies, namely the open-sintering (Fig. 1(a)), cover-sintering (Fig. 1(b)), and embed-sintering (Fig. 1(c)), were attempted. The open-sintering and the embed-sintering methods are considered to maintain the lowest and highest BaO activity, respectively. The BZY20–70 wt% NiO pellet-like samples were heated at 1500 °C for desired time (0, 2, 5, and 10 h) with a subsequent quench in the ambient atmosphere.

Both the mixtures containing BZY20 finally heating at 1300 and 1600 °C were examined here, but in general, these two samples behaved in a similar way, because the heat treatment temperature is 1500 °C. With the open-sintering method, as shown in Fig. 14(a) and (b), BaY_2NiO_5 existed even the samples were just heated up to 1500 °C (0 h), but the peak intensity of BaY_2NiO_5 decreased with the increasing heating time. Meanwhile, the peaks belonging to Y_2O_3 appeared when the sample was kept at 1500 °C for 2 h with its intensity increased with the time. Such phenomenon indicates that BaY_2NiO_5 formed during the elevating of temperature, but gradually decomposed during the static heating at 1500 °C. A quite similar result was obtained by using the cover-sintering method, as shown in Fig. 14(c) and (d). But it is worth noting here that a delayed rising of Y_2O_3 peak occurred with the cover-sintering method (2 h for the open-sintering method, but 5 h for the cover-sintering method).

When the embed-sintering method was applied, as shown in Fig. 14(e) and (f), peaks belonging to BaY_2NiO_5 were observed

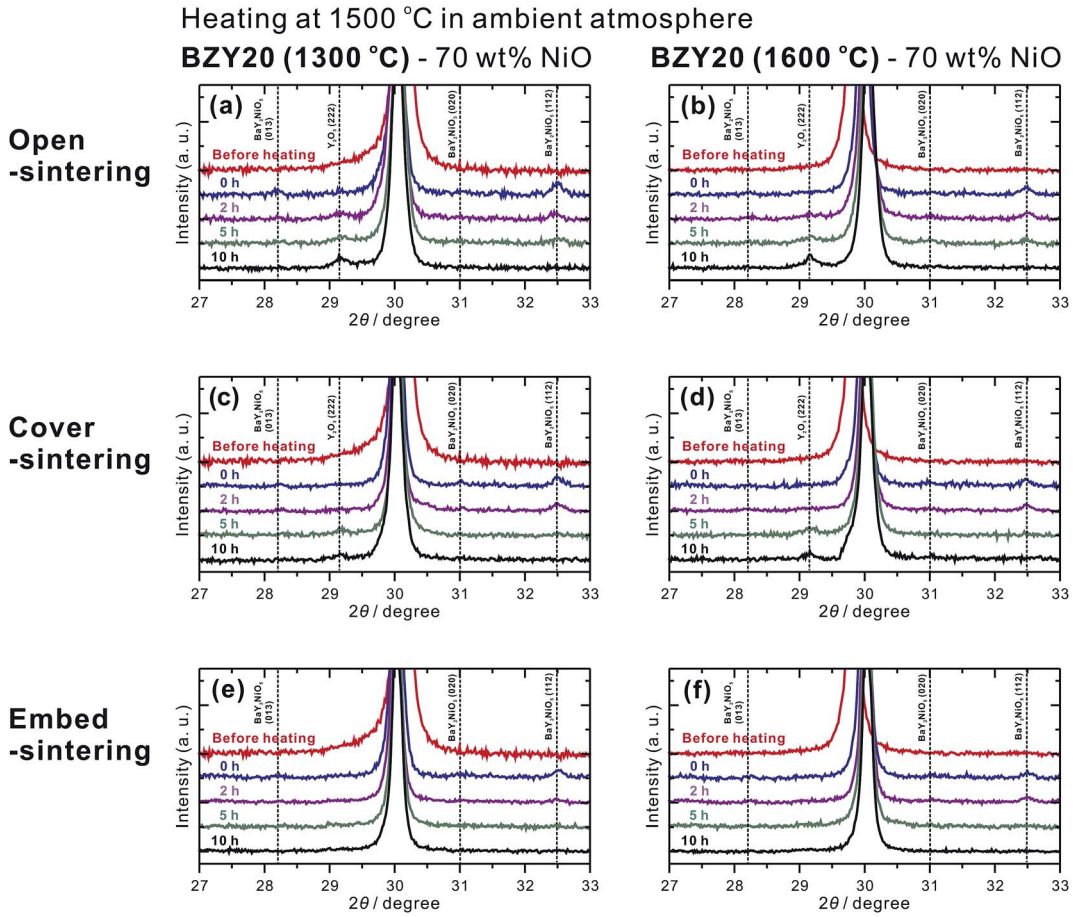

Fig. 14 Variation of powder XRD patterns (27–33 degree) for mixture of BZY20–70 wt% NiO heating at 1500 °C in ambient atmosphere for various time using three different sintering methods, namely, open-sintering (Fig. 1(a)), cover-sintering (Fig. 1(b)), and embed-sintering (Fig. 1(c)) methods. The BZY20 powder added was finally heat-treated at 1300 °C in ambient atmosphere for 10 h, or 1600 °C in O_2 for 24 h. The sharp peak around 30 degree is the (011) diffraction peak of BZY20. The heating rates in the temperature ranges of room temperature to 1000 °C, and 1000 °C to 1500 °C were 4.17 and 3.33 °C min^{-1}, respectively. All the samples were finally quenched in ambient atmosphere.

after just heating up to 1500 °C, but became weakened and finally disappeared after keeping at 1500 °C for 2 and 5 h, respectively (see a peak around 32.5°). It is especially interesting to see that Y_2O_3 was not observed, regardless of the heating time. No second phase appeared when the sample was kept at 1500 °C for 5 and 10 h. The results imply that relatively high BaO vapor assists incorporation of Y_2O_3 into the perovskite phase. These results indicate that controlling BaO activity is important.

4. Discussion

Tong *et al.* suggested that the melting point of BaY_2NiO_5 was between 1450 and 1500 °C.[17] However, in this work, we confirmed that BaY_2NiO_5 to be a solid phase at 1500 °C. But it is unstable due to the evaporation of oxides and hydroxides of barium and nickel at such high temperature. Furthermore, at 1600 °C, BaY_2NiO_5 peritectically decomposed to Y_2O_3 and a liquid phase. Anyhow, remaining of BaY_2NiO_5 in the fuel cells seems to be rather problematic, since it decomposes in the hydrogen atmosphere at 600 °C, which is an expected temperature for the BZY20 electrolyte-based fuel cell to operate.

In the anode, BaY_2NiO_5 formed due to the reaction between NiO and BZY20, which is revealed in this work to be a rather sophisticated process depending on a couple of parameters. Especially, the status of BZY20 after synthesizing is a very important factor. BZY20 which is relatively poor in homogeneity, and contains residue of raw materials ($BaCO_3$, Y_2O_3) exhibited high reactivity with NiO to maintain a wide temperature range for BaY_2NiO_5 to exist. However, a positive effect on suppressing the BaY_2NiO_5 formation was achieved by improving the compositional homogeneity of BZY20. Such improvement can be simply realized by just elevating the final heating temperature of BZY20 (namely, from 1300 °C to 1600 °C, in this study).

The sintering strategy, or the BaO activity during sintering in another word, also impacts greatly the phase appearance in the BZY20–NiO mixture. With the open-sintering (Fig. 1(a)) and cover-sintering (Fig. 1(b)) methods, which have relatively low BaO activity, Y_2O_3 was identified to be the only second phase after keeping at 1500 °C for 10 h. Such Y_2O_3 is considered to be generated from the decomposition of BaY_2NiO_5 residue formed at the low temperature range during the heating up process, because as shown in Fig. 14, BaY_2NiO_5 already existed in the sample just heated up to 1500 °C. We then increased the BaO activity during sintering by using the embed-sintering method (Fig. 1(c)), and was excited to see that the segregation of Y_2O_3 did not occur. Furthermore, there is even no second phase identified from XRD measurements after heating at 1500 °C for 5 and 10 h. It seems that Y, and possibly also Ni, return to the crystal lattice of barium zirconate, if a properly sufficient BaO activity can be supplied during the sintering.

5. Conclusions

The results in this work revealed that BaY_2NiO_5 was unstable at high temperature (1500 and 1600 °C) in a different way, and also in a reducing atmosphere at 600 °C. Remaining of BaY_2NiO_5 as a second phase in BZY20-based fuel cells seems quite problematic. A systematic work was therefore performed to provide fundamental insight into the reactivity between BZY20 and NiO. It was found that improving the compositional homogeneity of BZY20 powder, which was used in composing the electrolyte and anode layers, reduced or even suppressed effectively the formation of BaY_2NiO_5. It is rather interesting that such improvement in the compositional homogeneity can be yielded simply by just elevating the final heating temperature for BZY20, such as from 1300 to 1600 °C. Furthermore, a proper BaO activity in the environment during the sintering is another key factor, which can be adjusted by choosing appropriate sintering method. Improving the compositional homogeneity of BZY20, and controlling precisely the BaO activity, therefore provide a potential strategy to prepare a BZY20 electrolyte-based fuel cell without second phases.

Acknowledgements

The authors want to thank Mr Kenji Kazumi for STEM-EDS analysis.

References

1 Y. Yamazaki, R. Hernandez-Sanchez and S. M. Haile, *Chem. Mater.*, 2009, **21**, 2755.
2 D. Pergolesi, E. Fabbri, A. D'Epifanio, E. D. Bartolomeo, A. Tebano, S. Sanna, S. Licoccia, G. Balestrino and E. Traversa, *Nat. Mater.*, 2010, **9**, 846.
3 D. Han, K. Shinoda, S. Sato, M. Majima and T. Uda, *J. Mater. Chem. A.*, 2015, **3**, 1243.
4 R. M. Ormerod, *Chem. Soc. Rev.*, 2003, **32**, 17.
5 A. J. Jacobson, *Chem. Mater.*, 2010, **22**, 660.
6 Y. Okumura, Y. Nose, J. Katayama and T. Uda, *J. Electrochem. Soc.*, 2011, **158**, B1067.
7 J. Shim, J. Park, J. An, T. M. Gür, S. Kang and F. B. Printz, *Chem. Mater.*, 2009, **21**, 3290.
8 Y. Guo, Y. Lin, R. Ran and Z. Shao, *J. Power Sources*, 2009, **193**, 400.
9 W. Sun, L. Yan, Z. Shi, Z. Zhu and W. Liu, *J. Power Sources*, 2010, **195**, 4277.
10 L. Bi, E. Fabbri, Z. Sun and E. Traversa, *Energy Environ. Sci.*, 2011, **4**, 409.
11 L. Bi, E. Fabbri, Z. Sun and E. Traversa, *Energy Environ. Sci.*, 2011, **4**, 1352.
12 D. Pergolesi, E. Fabbri and E. Traversa, *Electrochem. Commun.*, 2010, **12**, 977.
13 C. Duan, J. Tong, M. Shang, S. Nikodemski, M. Sanders, S. Ricote, A. Almansoori and R. O'Hayre, *Science*, 2015, **349**, 1321.
14 L. Bi, E. Fabbri, Z. Sun and E. Traversa, *J. Electrochem. Soc.*, 2011, **158**, B797.
15 S. Fang, S. Wang, K. S. Brinkman, Q. Su, H. Wang and F. Chen, *J. Power Sources*, 2015, **278**, 614.
16 N. Narendar, G. C. Mather, P. A. N. Dias and D. P. Fagg, *RSC Adv.*, 2012, **3**, 859.

17 J. Tong, D. Clark, L. Bernau, M. Sanders and R. O'Hayre, *J. Mater. Chem.*, 2010, **20**, 6333.
18 D. Han, K. Shinoda, S. Tsukimoto, H. Takeuchi, C. Hiraiwa, M. Majima and T. Uda, *J. Mater. Chem. A*, 2014, **2**, 12552.
19 M. W. Chase Jr, *NIST-JANAF Thermochemical Tables, 4th ed., Part II; Journal of Physical and Chemical Reference Data, Monograph 9*, American Chemical Society, American Institute of Physics, Washington, 1998.
20 I. Barin, *Thermochemical Data of Pure Substances*, VCH Verlagsgesellschaft mbH, Weinheim, 1995.
21 A. D. Mah and L. B. Pankratz, *Contributions to the Data on Theoretical Metallurgy: XVI. Thermodynamic Properties of Nickel and Its Inorganic Compounds*, U.S. Bureau of Mines, Washington, 1976.
22 J. J. Lander, *J. Am. Chem. Soc.*, 1951, **73**, 2450.
23 D. J. Buttrey, J. D. Sullivan and A. L. Rheingold, *J. Solid State Chem.*, 1990, **88**, 291.
24 W. Zhang and K. Osamura, *Mater. Trans.*, 1991, **32**, 1048.
25 S. Imashuku, T. Uda, Y. Nose and Y. Awakura, *J. Phase Equilib. Diffus.*, 2010, **31**, 348.
26 C. Hiraiwa, D. Han, A. Kuramitsu, A. Kuwabara, H. Takeuchi, M. Majima and T. Uda, *J. Am. Ceram. Soc.*, 2013, **96**, 879.
27 D. Han, K. Kishida, K. Shinoda, H. Inui and T. Uda, *J. Mater. Chem. A*, 2013, **1**, 3027.
28 S. Imashuku, T. Uda, Y. Nose, G. Taniguchi, Y. Ito and Y. Awakura, *J. Electrochem. Soc.*, 2009, **156**, B1.
29 F. Giannici, M. Shirpour, A. Longo, A. Martorana, R. Merkle and J. Maier, *Chem. Mater.*, 2011, **23**, 2994.
30 Y. Oyama, A. Kojima, X. Li, R. B. Cervera, K. Tanaka and S. Yamaguchi, *Solid State Ionics*, 2011, **197**, 1.
31 M. Shirpour, R. Merkle and J. Maier, *Solid State Ionics*, 2012, **225**, 304.
32 D. Han, Y. Nose, K. Shinoda and T. Uda, *Solid State Ionics*, 2012, **213**, 2.
33 S. Fang, S. Wang, K. S. Brinkman and F. Chen, *J. Mater. Chem. A*, 2014, **2**, 5825.